

## The formation of heavy, radio-quiet neutron star binaries and the origin of GW190425

ALEJANDRO VIGNA-GÓMEZ,<sup>1</sup> SOPHIE L. SCHRÖDER,<sup>1</sup> ENRICO RAMIREZ-RUIZ,<sup>2,1</sup> DAVID R. AGUILERA-DENA,<sup>3,4,5</sup>  
ALDO BATTÀ,<sup>6</sup> NORBERT LANGER,<sup>4,5</sup> AND REINHOLD WILLCOX<sup>7,8</sup>

<sup>1</sup>*DARK, Niels Bohr Institute, University of Copenhagen, Jagtvej 128, 2200, Copenhagen, Denmark*

<sup>2</sup>*Department of Astronomy and Astrophysics, University of California, Santa Cruz, CA 95064, USA*

<sup>3</sup>*Institute of Astrophysics, FORTH, Dept. of Physics, University of Crete, Voutes, University Campus, GR-71003 Heraklion, Greece*

<sup>4</sup>*Argelander-Institut für Astronomie, Universität Bonn, Auf dem Hügel 71, 53121 Bonn, Germany*

<sup>5</sup>*Max-Planck-Institut für Radioastronomie, Auf dem Hügel 69, 53121 Bonn, Germany*

<sup>6</sup>*Instituto Nacional de Astrofísica, Óptica y Electrónica, Tonantzintla, Puebla 72840, México*

<sup>7</sup>*School of Physics and Astronomy, Monash University, Clayton, Vic. 3800, Australia*

<sup>8</sup>*The ARC Centre of Excellence for Gravitational Wave Discovery – OzGrav*

### ABSTRACT

The detection of the unusually heavy binary neutron star merger GW190425 marked a stark contrast to the mass distribution from known Galactic millisecond pulsars in neutron star binaries and gravitational-wave source GW170817. We suggest here a formation channel for heavy binary neutron stars in which massive helium stars, assembled after common envelope, remain compact and avoid mass transfer onto the neutron star companion and thus evade pulsar recycling. In particular we present three-dimensional simulations of the supernova explosion of the massive stripped helium star and follow the mass fallback evolution and the subsequent accretion onto the neutron star companion. We find that fallback leads to significant mass growth in the newly formed neutron star and that the companion does not accrete sufficient mass to become a millisecond pulsar. This can explain the formation of heavy binary neutron star systems such as GW190425, as well as predict the assembly of neutron star - light black hole systems. Moreover, this hints to the existence of a sizable population of radio-quiet double compact objects in our Galaxy. Finally, this formation avenue is consistent with the observed mass-eccentricity correlation of binary neutron stars in the Milky Way.

### 1. INTRODUCTION

On April 25th, 2019, the LIGO-Virgo network detected its second-ever signal of two neutron stars merging, tagged as GW190425 (Abbott et al. 2020). But unlike the first detection of a binary neutron star merger (GW170817, Abbott et al. 2017b), which conformed to expectations, GW190425 was extraordinary. Most of what we know about neutron stars comes primarily from observations of pulsars, magnetized rotating neutron stars, in our own Milky Way. Of the thousands of known pulsars, almost twenty are visible as recycled millisecond pulsars paired with another neutron star companion (Tauris et al. 2017; Andrews & Mandel 2019). These light neutron star binaries, including GW170817, weighed the equivalent of about 2.6 solar masses (Kiziltan et al. 2013; Özel & Freire 2016; Farrow et al. 2019).

By contrast, GW190425 has a total mass equal to about 3.4 solar masses (Abbott et al. 2020).

Since the detection of the Hulse–Taylor binary (Hulse & Taylor 1975), there is consensus that the progenitors of binary neutron stars are massive stellar binaries (e.g., van den Heuvel 1976). A crucial phase in the evolutionary pathway to binary neutron star formation occurs when a giant star fills its Roche lobe and initiates a dynamically-unstable mass-transfer episode onto the neutron star companion (e.g., Bhattacharya & van den Heuvel 1991). The stellar core and the neutron star become engulfed by the expanding envelope, a process where gas drag dissipates orbital energy of the binary (e.g., Ivanova et al. 2013; MacLeod & Ramirez-Ruiz 2015). This common envelope phase ends when the hydrogen envelope is ejected and a compact, stripped, helium-rich star of a few solar masses is left to reside in a tight ( $\approx R_{\odot}$ ) near circular orbit (Fragos et al. 2019; Law-Smith et al. 2020). The subsequent evolution of the binary (Figure 1) depends on the mass and composition of the stripped helium star (Woosley 2019) after the en-

velope is ejected. Most low-mass helium stars expand (e.g., Woosley et al. 1995; Götzberg et al. 2017; Laplace et al. 2020) and engage in an additional stable mass-transfer episode. During this episode, the mass transferred from the helium-rich donor recycles the pulsar, a process in which the neutron star spin increases to milliseconds and becomes radio visible for several Gyr (e.g., Srinivasan 2010). Moreover, the donor star becomes an ultra-stripped core (Tauris et al. 2013, 2015). These low-mass systems lead to binary neutron stars such as GW170817 and those observed in the Milky Way (e.g., Ramirez-Ruiz et al. 2019).

In this *Letter* we propose an alternative channel formation channel for heavy binary neutron stars. In this formation channel, massive ( $\gtrsim 9 M_{\odot}$ ) helium stars remain compact and avoid mass transfer onto a neutron star and thus pulsar recycling. Non-recycled, young, pulsars become radio quiet after only tens of Myr (e.g., Lorimer & Kramer 2004; Tauris et al. 2017) and, as a result, these massive helium stars lead to radio-quiet compact binaries that can only be detected by gravitational-wave observatories. The structure of the helium star at core collapse will determine if the system will become a binary neutron star or neutron star - black hole binary. These systems offer an alternative evolutionary pathway which can explain the dichotomy between the observed binary neutron stars hosting recycled pulsars, GW170817, and the unusually heavy gravitational-wave source GW190425 (Figure 1).

## 2. METHODS AND INITIAL CONDITIONS

In this *Letter* we present three-dimensional (3D) hydrodynamic models of GW190425-like progenitor systems using the smoothed-particle hydrodynamics (SPH) code GADGET-2 (Springel 2005). To generate our initial models we make use of the one-dimensional (1D) stellar evolution code MESA (Paxton et al. 2011) version 10398. In particular, we model the evolution of a  $10.0 M_{\odot}$  stripped star at  $Z = 0.02$  from helium zero-age main sequence to core collapse. At core collapse, the heavy helium star has a mass of  $M_{\text{pre-SN}} \approx 5.4 M_{\odot}$ , a radius of  $\approx 0.7 R_{\odot}$ , and more than 95% of its gravitational binding energy contained below a radius of  $0.01 R_{\odot}$ . The reader is refer to Appendix A for specifics. We then map the MESA model into GADGET-2 in order to simulate the supernova explosion of a heavy helium star with a  $1.3 M_{\odot}$  neutron star companion at a separation of  $a_{\text{pre-SN}} = 1.4 R_{\odot}$  in a circular orbit. Details on the setup and numerical tests can be found in Appendix B. The initial proto-neutron-star mass is assumed to be  $M_{\text{proto-NS}} = 1.3 M_{\odot}$ , consistent with the observed mass distribution of binary neutron stars

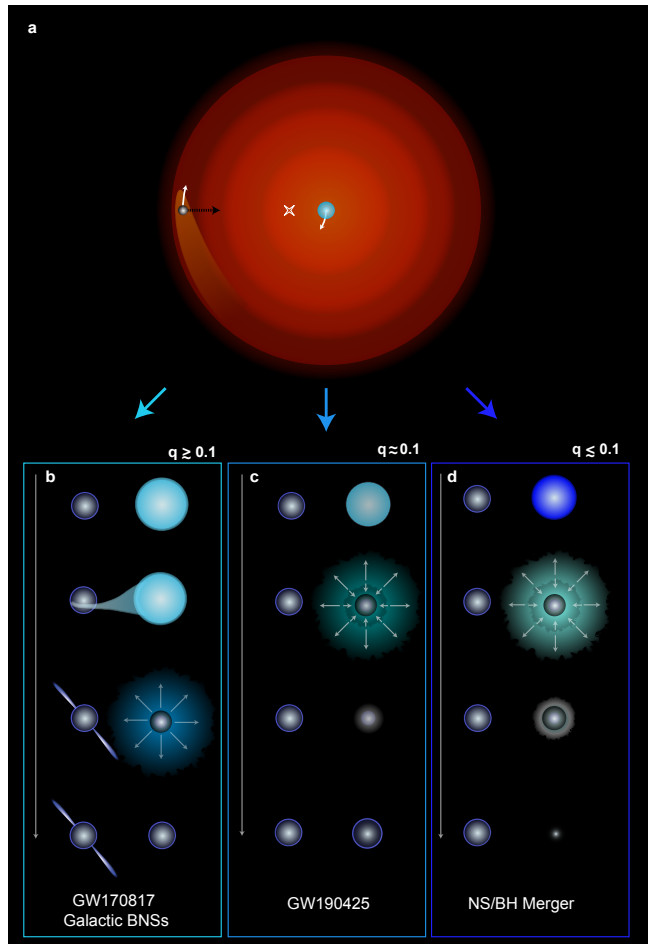


**Figure 1.** Late stages of binary neutron star formation. The giant star expands and engulfs the neutron star companion in an stage commonly referred to as a common-envelope evolution (a). A successful ejection of the envelope leaves the neutron star in a close orbit with a stripped-envelope star. The evolution of the system depends on the mass ratio  $q = M_{\text{NS}}/M_{\text{stripped}}$ . Less-massive stripped stars with  $q \gtrsim 0.1$  experience an additional mass transfer phase that further strips the star and recycles the pulsar companion. Such evolutionary sequence leads to systems such as the observed binary neutron stars in the Milky Way and GW170817 (b). More massive stripped stars with  $q \approx 0.1$  do not expand as much, therefore avoiding further stripping and companion recycling. Such evolutionary sequence, on the other hand, is expected to lead to binary neutron star systems such as GW190425 (c). Finally, even more massive stripped stars with  $q \lesssim 0.1$  will lead to neutron star - black hole binaries (d).

(Kiziltan et al. 2013; Özel & Freire 2016; Farrow et al. 2019) and with the properties of the 1D pre-supernova stellar model (Müller et al. 2016). An explosion en-

ergy of 1.5 bethes<sup>1</sup>, consistent with estimates from a 1D neutrino-hydrodynamics code for a similar progenitor model (Ertl et al. 2020), is deposited in a shell above the proto-neutron star. We focus on the long-term, post-explosion fallback evolution of the ejecta in order to account for mass accretion of the newly born neutron star and for pulsar recycling of the companion.

### 3. NEUTRON STAR BIRTH FROM SN FALLBACK

The resultant hydrodynamical evolution of the explosion is depicted in Figure 2. The shock initially propagates through the iron core until it reaches the envelope, fractions of a second after the explosion. At this point, a reverse shock wave emerges, which propagates back towards the newly-formed neutron star and triggers mass fallback. The fallback mass accretion rate peaks 20 s after the explosion at  $\approx 10^{-2} M_{\odot} \text{ s}^{-1}$  (Figure 2). Approximately  $0.8 M_{\odot}$  are accreted during the first hundred seconds after the explosion, roughly the same time scale in which the expanding layers of the exploding star reach the neutron star companion (Figure 2). The rapid velocity of the expanding shock ( $\approx 1000 \text{ km s}^{-1}$ ) and the small cross section of the neutron star companion result in  $\lesssim 10^{-3} M_{\odot}$  of accreted material. The accretion of this small amount of material will not effectively recycle the neutron star companion (e.g., Tauris et al. 2017).

After thousands of seconds the newly formed neutron star approaches a final mass of  $\approx 2.1 M_{\odot}$ , a value in broad agreement with earlier results (Fryer et al. 2012; Ertl et al. 2020) in the literature. During the whole simulation the accretion rate remains above hypercritical (Chevalier 1993) and neutrinos provide the main cooling mechanism until after  $\approx 10^6 \text{ s}$ .

The amount of fallback mass accretion increases with decreasing explosion energy (Figure 3). Energies of  $E_{\text{exp}} \lesssim 0.5$  bethes lead to almost complete fallback while explosion energies of  $E_{\text{exp}} \gtrsim 2.5$  bethes lead to a complete ejection of the envelope. The fallback-dominated transition from neutron star to black hole remnants occurs at  $E_{\text{exp}} \lesssim 1.3$  bethes. Explosion energies between  $1.3 \lesssim E_{\text{exp}} \lesssim 2.4$  bethes lead to remnant masses  $1.6 \lesssim M_{\text{rem,exp}}/M_{\odot} \lesssim 2.7$ , which are in the inferred range for the heavy neutron star in GW190425 (Abbott et al. 2020). Future detections of binary neutron stars and neutron star - black hole binaries would thus help improve the so far weak constraints of supernova explosion energies from massive helium stars.

The ejected envelope material during a supernova explosion imparts a recoil kick on the system. Even if the supernova is spherically-symmetric in the frame of ref-

erence of the exploding star, the explosion will increase the orbital period and eccentricity (Blaauw 1961). If, on the other hand, the supernova material is ejected anisotropically, the magnitude of the resultant kick to the newly born neutron star is expected to be of the order of  $\approx 100 \text{ km s}^{-1}$  for isolated massive stars (e.g., Burrows & Vartanyan 2021) and reduced to  $\approx 10 \text{ km s}^{-1}$  for ultra-stripped or electron-capture supernovae (e.g., Vigna-Gómez et al. 2018). Binary neutron stars assembled via common-envelope episodes end up in close orbits with relative orbital velocities well in excess of  $1000 \text{ km s}^{-1}$  and are likely to remain gravitationally bound after the explosion. Depending on the direction and magnitude of the natal kick, some binaries might actually end up shrinking to even closer orbits. The explosion of massive helium stars with a light neutron star companion are expected to lead to the formation of more eccentric binaries. Only close pre-supernova binaries ( $\lesssim 5 R_{\odot}$ ) can give rise to binary neutron stars that can merge within the age of the Universe (Figure 4).

## 4. DISCUSSION AND CONCLUSIONS

### 4.1. Rates

The rates for this binary neutron star formation channel depend sensitively on the mass and metallicity of the helium star progenitor. Expanding helium stars, which engage in mass transfer and recycle the pulsar companion, become ultra-stripped progenitors (Tauris et al. 2013) of  $\approx 1.3 - 1.4 M_{\odot}$  neutron stars. This is a commonly discussed formation avenue of binary neutron stars in the Milky Way (e.g., Tauris et al. 2017; Vigna-Gómez et al. 2018) and the first binary neutron star merger GW170817 (Abbott et al. 2017b; Vigna-Gómez et al. 2018; Kruckow et al. 2018). On the other hand, more massive helium stars can form heavy neutron stars or even black holes via fallback accretion. We use rapid population synthesis (Appendix C) to estimate the amount of potential *systems of interest*. We define systems of interest as stars that engage in a common-envelope phase with a neutron star companion, that could assemble either radio-quiet heavy binary neutron star or neutron star - black hole binaries.

At any metallicity, the yield of these systems of interest is  $\approx 10^{-5} M_{\odot}^{-1}$ , which results in a local birth rate upper limit of  $\approx 100 \text{ Myr}^{-1}$  (Appendix C and Figure 10). Stars with sub-solar metallicity have diminished mass loss rates, lead to a larger fraction of massive helium cores, and are more compact than their higher metallicity counterparts. In the case of GW190425, the host galaxy, environment, and the metallicity of the circumbinary merger environment remains elusive given that no electromagnetic counterpart was detected (Hos-

<sup>1</sup> 1 bethe :=  $10^{51}$  erg.

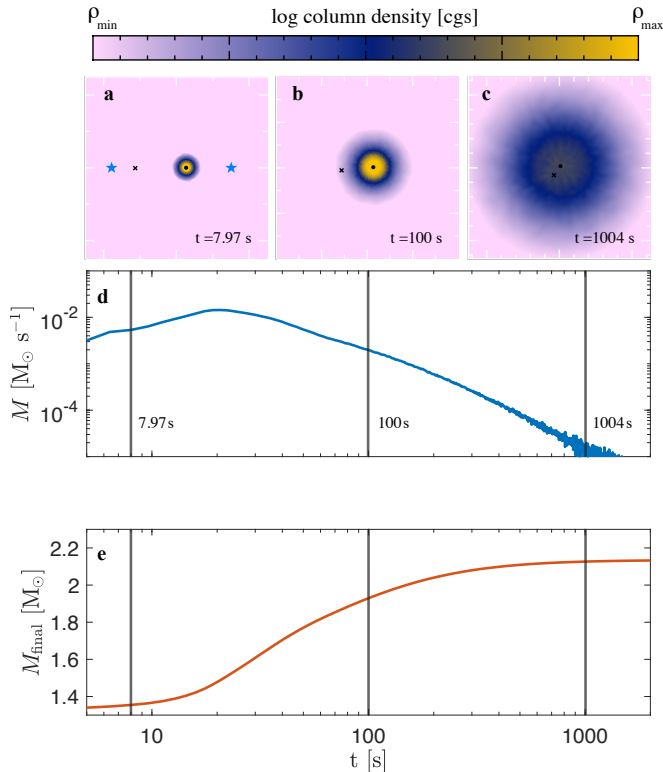


**Figure 2.** The hydrodynamical evolution of the second supernova and the accompanying mass fallback that leads to a heavy binary neutron star merger. Panels (a)-(c) show the column density (cgs units) in base 10 logarithmic scale and span  $[-1,3]$  in (a),  $[-2,2]$  in (b) and  $[-3,1]$  in (c). The location of the newly born neutron star is shown as a filled black circle and the companion neutron star is shown as a black cross. The second and third outer Lagrangian points of the binary are shown as blue stars in panel (a). The tick marks on each panel correspond to a solar-radius scale. The only interaction with the neutron star companion is from the blasted ejecta and there is only a tiny mass of material accreted, implying that the pulsar companion will not be effectively recycled. Panels (d) and (e) show the fallback mass accretion rate onto the newly born neutron star and its cumulative mass accretion growth, both with vertical lines marking the snapshots from panels (a)-(c).

seinzadeh et al. 2019). More precise merger rates of heavy binary neutron stars and neutron star - black hole mergers can be calculated by incorporating *state-of-the-art* models of stripped stars (Appendix A) to population synthesis calculations. We plan to explore this in future work.

#### 4.2. Mass-eccentricity correlation

There are hints of a mass-eccentricity correlation in short period ( $< 1$  day) binary neutron stars in the Milky Way, where millisecond pulsars paired with more massive companions ( $\approx 1.4 M_{\odot}$ ) are in more eccen-

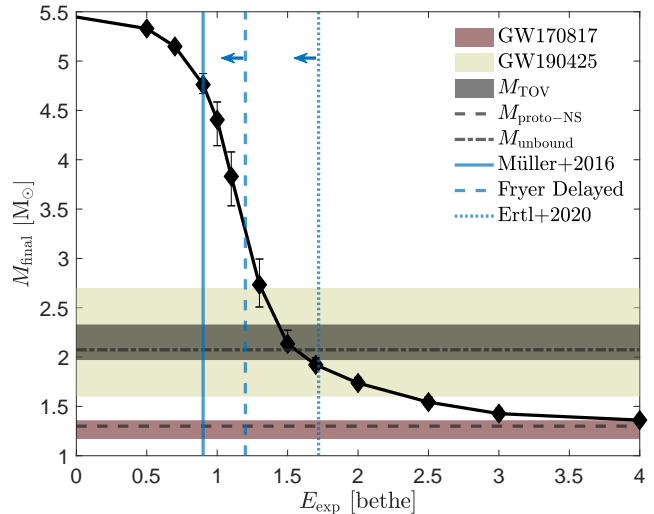


**Figure 3.** Mass of the newly formed remnant as a function of the supernova explosion energy after the fallback accretion has ceased. The range of the component mass for gravitational-wave sources GW170817 and GW190425 is shown in pink and beige, respectively, while the maximum mass of a non-rotating neutron star,  $M_{\text{TOV}}$  (Rezzolla et al. 2018), in shown in grey. The proto-neutron-star (proto-NS) mass of  $1.3 M_{\odot}$ , same as the neutron star companion, is shown as a black dashed line. For this configuration, if  $\approx 3.4 M_{\odot}$  are symmetrically ejected during the supernova, the binary becomes gravitationally unbound. The semi-analytical prediction (Müller et al. 2016) of the explosion energy for this particular model is shown as a solid blue line. The upper limits of supernova models with explosion energies which include fallback are shown as dashed and dotted blue lines (Fryer et al. 2012; Ertl et al. 2020). Main numerical uncertainties are included as error bars, some of them within the symbols (Appendix B).

tric ( $\approx 0.6$ ) orbits (e.g., Tauris et al. 2017; Andrews & Mandel 2019). The formation channel proposed here for GW190425 is consistent with this trend and suggests that heavy binary neutron stars can be highly eccentric at birth and still merge within the age of the Universe (Figure 4). The fallback scenario presented here thus provides an explanation for the observed mass-eccentricity correlation without the need to rely on a dynamical-formation scenario (Andrews & Mandel 2019). To date, there is no evidence of heavy ( $> 2.9 M_{\odot}$ ) binary neutron stars in the Milky Way. This suggests at least one of the following three things about heavy binary neutron stars: they have very short orbital periods ( $\lesssim$  few hours) and thus avoid detection in acceleration searches (Abbott et al. 2020; Safarzadeh et al. 2020; Galaudage et al. 2021), they are radio quiescent, or such systems are extremely rare in the Milky Way



(Galadage et al. 2021). A priori, there is no reason why heavy binary neutron stars should be preferentially born in short orbital periods (but see Romero-Shaw et al. 2020) and standard formation models are unable to predict enough fast mergers to be reconciled with the detection of GW190425 (Safarzadeh et al. 2020).

#### 4.3. Electromagnetic counterparts

The merger of a heavy neutron star pair or a neutron star - light black hole binary is expected to produce an electromagnetic counterpart that will further shed light on its origin (Roberts et al. 2011). Particularly, the merger of a heavy neutron star pair is expected to produce a luminous red kilonova likely powered by an accretion disk wind (Kasen et al. 2017), which might likely be accompanied by a blue kilonova component (Metzger & Fernández 2014). The merger of a neutron star - light black hole binary, on the other hand, is expected to experience tidal disruption and be only observable as faint red kilonova (Kasen et al. 2017). The accompanying electromagnetic signatures would provide a natural test to distinguish between different compact binary mergers.

#### 4.4. LISA

The formation channel presented here strongly hints to the presence of heavy, radio-quiet neutron star binaries and in the Milky Way. These and similar systems, such as non-recycled light binary neutron stars (Belczyński & Kalogera 2001) and neutron stars with light black hole companions, are expected to be uncovered by the Laser Interferometer Space Antenna (Amaro-Seoane et al. 2017; Lau et al. 2020).

#### 4.5. Conclusions

Our understanding of merging binaries has come a long way since the discovery of gravitational waves almost 6 years ago, but these enigmatic sources continue to offer major puzzles and challenges. Our results suggest that ground-based facilities, like LIGO and Virgo, will detect these merging binary populations which have currently avoided detection in the Milky Way. Space- and ground-based observations over the coming decade should allow us to uncover the detailed nature of these most remarkable systems and provide us with an exciting opportunity to study novel regimes of binary stellar evolution.

The authors thank Ilya Mandel and Simon Stevenson for useful discussions. A.V.-G., S.L.S., and E.R.-R. acknowledge support by Heising-Simons Foundation, the Danish National Research Foundation (DNRF132) and

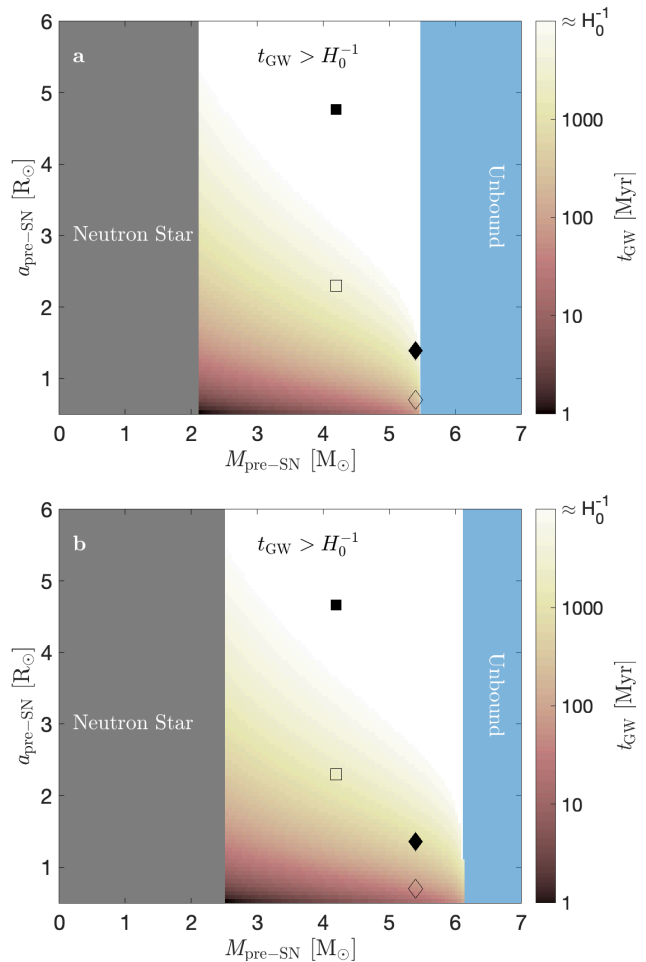


**Figure 4.** Time to binary neutron star merger via gravitational-wave emission for different pre-supernova orbital configurations. Panel (a) is for a circular binary with a spherically symmetric explosion leaving a  $2.1 M_{\odot}$  remnant with a  $1.3 M_{\odot}$  neutron star companion. The hollow symbols represent the radii of two different stellar models at core-collapse, where the more massive one (diamond) is more compact than the less massive one (square). The filled symbols represent the minimum separation needed so that the star avoids filling its Roche lobe. Only the more massive model (diamond) can lead to a binary neutron star merger within the age of the Universe ( $H_0^{-1}$ ). The blue region highlights unbound systems, where the ejected mass leads to a disruption of the binary. The gray region denotes the mass of the second neutron star for our fiducial model. Panel (b) is for a circular binary with a spherically symmetric explosion leaving a more massive  $2.5 M_{\odot}$  remnant with a  $1.3 M_{\odot}$  neutron star companion. Variations in the remnant mass, e.g., panel (a) vs (b), and the companion mass lead to different merger timescales.

NSF (AST-1911206 and AST-1852393). D. R. A.-D. was supported by the Stavros Niarchos Foundation (SNF) and the Hellenic Foundation for Research and Innovation (H.F.R.I.) under the 2nd Call of “Science and Society” Action Always strive for excellence – “Theodoros Papazoglou” (Project Number: 01431).

*Software:* Data and scripts used for this study available via [zenodo.org/record/4682798](https://zenodo.org/record/4682798). GADGET-2 is publicly available at <https://wwwmpa.mpa-garching.mpg.de/gadget/>. MESA is publicly available at <https://mesa.sourceforge.net>. COMPAS v02.19.01 publicly available at GitHub via [TeamCOMPAS/COMPAS](https://github.com/TeamCOMPAS/COMPAS). SPLASH is publicly available at <https://users.monash.edu.au/~dprice/splash/>.

## REFERENCES

- Abbott, B. P., Abbott, R., Abbott, T. D., et al. 2017a, ApJL, 848, L12, doi: [10.3847/2041-8213/aa91c9](https://doi.org/10.3847/2041-8213/aa91c9)
- . 2017b, PhRvL, 119, 161101, doi: [10.1103/PhysRevLett.119.161101](https://doi.org/10.1103/PhysRevLett.119.161101)
- . 2020, ApJL, 892, L3, doi: [10.3847/2041-8213/ab75f5](https://doi.org/10.3847/2041-8213/ab75f5)
- Aguilera-Dena, D. R., et al. in prep.
- Amaro-Seoane, P., Audley, H., Babak, S., et al. 2017, arXiv e-prints, arXiv:1702.00786, <https://arxiv.org/abs/1702.00786>
- Andrews, J. J., & Mandel, I. 2019, ApJL, 880, L8, doi: [10.3847/2041-8213/ab2ed1](https://doi.org/10.3847/2041-8213/ab2ed1)
- Batta, A., Ramirez-Ruiz, E., & Fryer, C. 2017, ApJL, 846, L15, doi: [10.3847/2041-8213/aa8506](https://doi.org/10.3847/2041-8213/aa8506)
- Belczyński, K., & Kalogera, V. 2001, ApJL, 550, L183, doi: [10.1086/319641](https://doi.org/10.1086/319641)
- Bhattacharya, D., & van den Heuvel, E. P. J. 1991, PhR, 203, 1, doi: [10.1016/0370-1573\(91\)90064-S](https://doi.org/10.1016/0370-1573(91)90064-S)
- Blaauw, A. 1961, BAN, 15, 265
- Böhm-Vitense, E. 1958, ZA, 46, 108
- Burrows, A., & Vartanyan, D. 2021, Nature, 589, 29, doi: [10.1038/s41586-020-03059-w](https://doi.org/10.1038/s41586-020-03059-w)
- Chevalier, R. A. 1993, ApJL, 411, L33, doi: [10.1086/186905](https://doi.org/10.1086/186905)
- Chomiuk, L., & Povich, M. S. 2011, AJ, 142, 197, doi: [10.1088/0004-6256/142/6/197](https://doi.org/10.1088/0004-6256/142/6/197)
- Ertl, T., Woosley, S. E., Sukhbold, T., & Janka, H. T. 2020, ApJ, 890, 51, doi: [10.3847/1538-4357/ab6458](https://doi.org/10.3847/1538-4357/ab6458)
- Everson, R. W., MacLeod, M., De, S., et al. 2020, ApJ, 899, 77, doi: [10.3847/1538-4357/aba75c](https://doi.org/10.3847/1538-4357/aba75c)
- Farrow, N., Zhu, X.-J., & Thrane, E. 2019, ApJ, 876, 18, doi: [10.3847/1538-4357/ab12e3](https://doi.org/10.3847/1538-4357/ab12e3)
- Fragos, T., Andrews, J. J., Ramirez-Ruiz, E., et al. 2019, ApJL, 883, L45, doi: [10.3847/2041-8213/ab40d1](https://doi.org/10.3847/2041-8213/ab40d1)
- Fryer, C. L., Belczynski, K., Wiktorowicz, G., et al. 2012, ApJ, 749, 91, doi: [10.1088/0004-637X/749/1/91](https://doi.org/10.1088/0004-637X/749/1/91)
- Galadage, S., Adamcewicz, C., Zhu, X.-J., Stevenson, S., & Thrane, E. 2021, ApJL, 909, L19, doi: [10.3847/2041-8213/abe7f6](https://doi.org/10.3847/2041-8213/abe7f6)
- Górski, K. M., Hivon, E., Banday, A. J., et al. 2005, ApJ, 622, 759, doi: [10.1086/427976](https://doi.org/10.1086/427976)
- Götberg, Y., de Mink, S. E., & Groh, J. H. 2017, A&A, 608, A11, doi: [10.1051/0004-6361/201730472](https://doi.org/10.1051/0004-6361/201730472)
- Hosseinzadeh, G., Cowperthwaite, P. S., Gomez, S., et al. 2019, ApJL, 880, L4, doi: [10.3847/2041-8213/ab271c](https://doi.org/10.3847/2041-8213/ab271c)
- Howitt, G., Stevenson, S., Vigna-Gómez, A., et al. 2020, MNRAS, 492, 3229, doi: [10.1093/mnras/stz3542](https://doi.org/10.1093/mnras/stz3542)
- Hulse, R. A., & Taylor, J. H. 1975, ApJL, 195, L51, doi: [10.1086/181708](https://doi.org/10.1086/181708)
- Ivanova, N., Justham, S., Chen, X., et al. 2013, A&A Rv, 21, 59, doi: [10.1007/s00159-013-0059-2](https://doi.org/10.1007/s00159-013-0059-2)
- Kasen, D., Metzger, B., Barnes, J., Quataert, E., & Ramirez-Ruiz, E. 2017, Nature, 551, 80, doi: [10.1038/nature24453](https://doi.org/10.1038/nature24453)
- Kiziltan, B., Kottas, A., De Yoreo, M., & Thorsett, S. E. 2013, ApJ, 778, 66, doi: [10.1088/0004-637X/778/1/66](https://doi.org/10.1088/0004-637X/778/1/66)
- Klencki, J., Nelemans, G., Istrate, A. G., & Chruslinska, M. 2021, A&A, 645, A54, doi: [10.1051/0004-6361/202038707](https://doi.org/10.1051/0004-6361/202038707)
- Kruckow, M. U. 2020, A&A, 639, A123, doi: [10.1051/0004-6361/202037519](https://doi.org/10.1051/0004-6361/202037519)
- Kruckow, M. U., Tauris, T. M., Langer, N., Kramer, M., & Izzard, R. G. 2018, MNRAS, 481, 1908, doi: [10.1093/mnras/sty2190](https://doi.org/10.1093/mnras/sty2190)
- Laplace, E., Götberg, Y., de Mink, S. E., Justham, S., & Farmer, R. 2020, A&A, 637, A6, doi: [10.1051/0004-6361/201937300](https://doi.org/10.1051/0004-6361/201937300)
- Lau, M. Y. M., Mandel, I., Vigna-Gómez, A., et al. 2020, MNRAS, 492, 3061, doi: [10.1093/mnras/staa002](https://doi.org/10.1093/mnras/staa002)
- Law-Smith, J. A. P., Everson, R. W., Ramirez-Ruiz, E., et al. 2020, arXiv e-prints, arXiv:2011.06630, <https://arxiv.org/abs/2011.06630>
- Lorimer, D. R., & Kramer, M. 2004, Handbook of Pulsar Astronomy, Vol. 4
- MacLeod, M. & Ramirez-Ruiz, E. 2015, ApJL, 798, L19, doi: [10.1088/2041-8205/798/1/L19](https://doi.org/10.1088/2041-8205/798/1/L19)
- Metzger, B. D. & Fernández, R. 2014, MNRAS, 441, 3444, doi: [10.1093/mnras/stu802](https://doi.org/10.1093/mnras/stu802)
- Müller, B., Heger, A., Liptai, D., & Cameron, J. B. 2016, MNRAS, 460, 742, doi: [10.1093/mnras/stw1083](https://doi.org/10.1093/mnras/stw1083)

- Ohlmann, S. T., Röpke, F. K., Pakmor, R., & Springel, V. 2017, *A&A*, 599, A5, doi: [10.1051/0004-6361/201629692](https://doi.org/10.1051/0004-6361/201629692)
- Özel, F., & Freire, P. 2016, *ARA&A*, 54, 401, doi: [10.1146/annurev-astro-081915-023322](https://doi.org/10.1146/annurev-astro-081915-023322)
- Paxton, B., Bildsten, L., Dotter, A., et al. 2011, *ApJS*, 192, 3, doi: [10.1088/0067-0049/192/1/3](https://doi.org/10.1088/0067-0049/192/1/3)
- Paxton, B., Cantiello, M., Arras, P., et al. 2013, *ApJS*, 208, 4, doi: [10.1088/0067-0049/208/1/4](https://doi.org/10.1088/0067-0049/208/1/4)
- Paxton, B., Marchant, P., Schwab, J., et al. 2015, *ApJS*, 220, 15, doi: [10.1088/0067-0049/220/1/15](https://doi.org/10.1088/0067-0049/220/1/15)
- Paxton, B., Schwab, J., Bauer, E. B., et al. 2018, *ApJS*, 234, 34, doi: [10.3847/1538-4365/aaa5a8](https://doi.org/10.3847/1538-4365/aaa5a8)
- Price, D. J. 2007, *PASA*, 24, 159, doi: [10.1071/AS07022](https://doi.org/10.1071/AS07022)
- Rezzolla, L., Most, E. R., & Weih, L. R. 2018, *ApJL*, 852, L25, doi: [10.3847/2041-8213/aaa401](https://doi.org/10.3847/2041-8213/aaa401)
- Ramirez-Ruiz, E., Andrews, J. J., & Schröder, S. L. 2019, *ApJL*, 883, L6, doi: [10.3847/2041-8213/ab3f2c](https://doi.org/10.3847/2041-8213/ab3f2c)
- Roberts, L. F., Kasen, D., Lee, W. H., & Ramirez-Ruiz, E. 2011, *ApJL*, 736, L21, doi: [10.1088/2041-8205/736/1/L21](https://doi.org/10.1088/2041-8205/736/1/L21)
- Romero-Shaw, I. M., Farrow, N., Stevenson, S., Thrane, E., & Zhu, X.-J. 2020, *MNRAS*, 496, L64, doi: [10.1093/mnras/rlaa084](https://doi.org/10.1093/mnras/rlaa084)
- Safarzadeh, M., Ramirez-Ruiz, E., & Berger, E. 2020, *ApJ*, 900, 13, doi: [10.3847/1538-4357/aba596](https://doi.org/10.3847/1538-4357/aba596)
- Schootemeijer, A., Langer, N., Grin, N. J., & Wang, C. 2019, *A&A*, 625, A132, doi: [10.1051/0004-6361/201935046](https://doi.org/10.1051/0004-6361/201935046)
- Schröder, S. L., Batta, A., & Ramirez-Ruiz, E. 2018, *ApJL*, 862, L3, doi: [10.3847/2041-8213/aacf8d](https://doi.org/10.3847/2041-8213/aacf8d)
- Springel, V. 2005, *MNRAS*, 364, 1105, doi: [10.1111/j.1365-2966.2005.09655.x](https://doi.org/10.1111/j.1365-2966.2005.09655.x)
- Srinivasan, G. 2010, *NewAR*, 54, 93, doi: [10.1016/j.newar.2010.09.026](https://doi.org/10.1016/j.newar.2010.09.026)
- Stevenson, S., Vigna-Gómez, A., Mandel, I., et al. 2017, *Nature Communications*, 8, 14906, doi: [10.1038/ncomms14906](https://doi.org/10.1038/ncomms14906)
- Tauris, T. M., Langer, N., Moriya, T. J., et al. 2013, *ApJL*, 778, L23, doi: [10.1088/2041-8205/778/2/L23](https://doi.org/10.1088/2041-8205/778/2/L23)
- Tauris, T. M., Langer, N., & Podsiadlowski, P. 2015, *MNRAS*, 451, 2123, doi: [10.1093/mnras/stv990](https://doi.org/10.1093/mnras/stv990)
- Tauris, T. M., Kramer, M., Freire, P. C. C., et al. 2017, *ApJ*, 846, 170, doi: [10.3847/1538-4357/aa7e89](https://doi.org/10.3847/1538-4357/aa7e89)
- Thorne, K. S., & Zytzkow, A. N. 1975, *ApJL*, 199, L19, doi: [10.1086/181839](https://doi.org/10.1086/181839)
- . 1977, *ApJ*, 212, 832, doi: [10.1086/155109](https://doi.org/10.1086/155109)
- van den Heuvel, E. P. J. 1976, in *Structure and Evolution of Close Binary Systems*, ed. P. Eggleton, S. Mitton, & J. Whelan, Vol. 73, 35
- Vigna-Gómez, A., Neijssel, C. J., Stevenson, S., et al. 2018, *MNRAS*, 481, 4009, doi: [10.1093/mnras/sty2463](https://doi.org/10.1093/mnras/sty2463)
- Vigna-Gómez, A., MacLeod, M., Neijssel, C. J., et al. 2020, *PASA*, 37, e038, doi: [10.1017/pasa.2020.31](https://doi.org/10.1017/pasa.2020.31)
- Vigna-Gómez, A., Aguilera-Dena, D. R., & Willcox, R. 2021, Dataset from: The formation of heavy, radio-quiet neutron star binaries and the origin of GW190425, Zenodo, doi: [10.5281/zenodo.4682798](https://doi.org/10.5281/zenodo.4682798), <https://doi.org/10.5281/zenodo.4682798>
- Woosley, S. E. 2019, *ApJ*, 878, 49, doi: [10.3847/1538-4357/ab1b41](https://doi.org/10.3847/1538-4357/ab1b41)
- Woosley, S. E., Langer, N., & Weaver, T. A. 1995, *ApJ*, 448, 315, doi: [10.1086/175963](https://doi.org/10.1086/175963)
- Yoon, S.-C., Dessart, L., & Clocchiatti, A. 2017, *ApJ*, 840, 10, doi: [10.3847/1538-4357/aa6afe](https://doi.org/10.3847/1538-4357/aa6afe)

## APPENDIX

## A. 1D EVOLUTION OF STRIPPED STARS.

We model the evolution of stripped stars using the 1D stellar evolution code MESA (Paxton et al. 2011) version 10398 (Paxton et al. 2013, 2015, 2018) as presented in Aguilera-Dena et al. (2021). We follow the evolution from helium zero-age main sequence until the onset of core collapse, which we define as the moment where core infall velocity is larger than  $1000 \text{ km s}^{-1}$ .

## A.1. Numerical setup.

The initial models are created by artificially mixing hydrogen-rich models from the pre-main-sequence phase, and until the beginning of helium burning. There is no mass loss until the beginning of helium burning, but the condition of homogeneity is relaxed at core nitrogen ignition; this guarantees the appropriate CNO element distribution (enhanced N, reduced C and O) for the stripped star. We follow Yoon et al. (2017) to account for mass loss through stellar winds, dependent on the stellar type (WN or WC) and metallicity. We use the `approx21` nuclear network and set resolution variables to `varcontrol_target=10-5`, and `mesh_delta_coef=0.5`, which results in a finer resolution than MESA’s default. Convection was modeled using standard mixing length theory (Böhm-Vitense 1958) with  $\alpha_{MLT} = 2.0$ , adopting the Ledoux criterion for instability, employing efficient semiconvection with  $\alpha_{SC} = 1.0$  (Schootemeijer et al. 2019), and using predictive mixing in the helium burning regions (Paxton et al. 2018). We use MESA’s `m1t++` for the treatment of energy transport in the envelope and neglect radiative acceleration in layers with  $T > 10^8 \text{ K}$  during late phases of evolution. This results in compact helium zero-age main sequence radius of  $\lesssim 1.2 R_{\odot}$ , and a minimum mass threshold of  $9.5 M_{\odot}$  for the  $Z = 0.02$  model. We do not include convective overshooting, which could result in larger core masses for initially less massive stars.

A.2. Evolution of two representative models at  $Z = 0.02$ .

The more massive model is initially  $10.0 M_{\odot}$  and reaches advanced stages of burning faster and collapses before being able to expand above its initial radius (Figure 6). Under pristine conditions, a  $10.0 M_{\odot}$  helium core corresponds to a zero-age main sequence mass of  $\approx 32.0 M_{\odot}$  (according to the models from Woosley 2019); however, the models presented here could have accreted matter via mass transfer episodes at some point in their lives. At the end of the evolution, this model has a very compact envelope that decreases sharply in density until reaching the outer layers (Figure 5). The less massive model is  $6.0 M_{\odot}$  and is computed to show the contrast with the more massive counterpart. If this less massive model is in a close binary, it is likely to experience a mass transfer episode. This less massive model is more similar to the canonical helium models that explain ultra-stripped stars, the progenitors of ultra-stripped supernovae, Galactic binary neutron stars and GW170817 (Tauris et al. 2013, 2015, 2017; Abbott et al. 2017b).

## A.3. Metallicity and mixing study.

There is a dichotomy between stripped stars that do or do not expand which is mass, model and metallicity dependent (Woosley 2019). To test the mass and metallicity dependence we performed calculations for helium zero-age main sequence masses between  $4.0 \leq M/M_{\odot} \leq 14.0$  in steps of  $0.5 M_{\odot}$  and at metallicities  $Z = \{0.010, 0.015, 0.020, 0.025, 0.030\}$  (Figure 7). These are a subset of the simulations done in Aguilera-Dena et al. (2021). Stripped stars have helium zero-age main sequence radii of  $\lesssim 1.5 R_{\odot}$  and are more compact at lower metallicities. In order to distinguish between stars which significantly expand and those which remain compact, we introduce a dimensionless factor  $R_{\text{final}}/R_{\text{He-ZAMS}}$ , where  $R_{\text{He-ZAMS}}$  is the radius at helium zero-age main sequence and  $R_{\text{final}}$  is the radius at the moment when the central carbon abundance is  $\lesssim 5 \times 10^{-3}$ , a proxy for central carbon depletion. Stars with  $R_{\text{final}}/R_{\text{He-ZAMS}} \lesssim 1$  remain compact. The minimum mass threshold to remain compact is  $9.0 M_{\odot}$  at  $Z = 0.02$ ; we use this value for the rate estimates (Appendix C). We test for alternative energy transport envelope treatment by turning off `m1t++` and allowing for radiative acceleration in the envelope. This variation results in helium zero-age main sequence radii of  $\lesssim 1.5 R_{\odot}$ , and mass threshold of  $10.0 M_{\odot}$  for the  $Z = 0.02$  model. The overall uncertainties on the minimum mass threshold are of order  $\lesssim 1.0 M_{\odot}$ .

## A.4. Some open questions in stellar binary evolution

The evolution from zero-age main sequence to double compact formation is rather complex. We have assumed here that the evolution of the system follows the canonical assembly of binary neutron stars (e.g., Bhattacharya & van



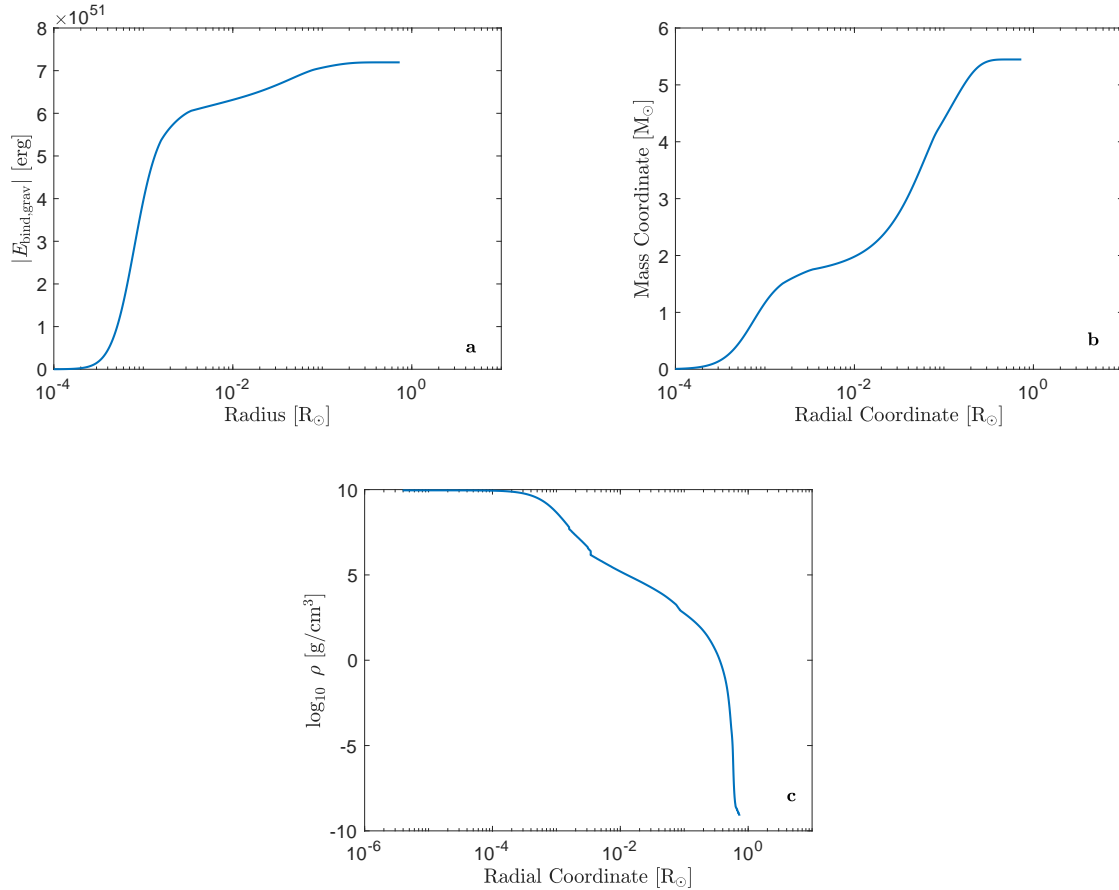


**Figure 5. Stellar structure of exploding model at the onset of core collapse.** Gravitational binding energy (a), mass coordinate (b) and density (c) as a function of radial coordinate for the models with helium zero-age main sequence mass of  $10.0 M_{\odot}$  at metallicity  $Z = 0.02$ .

den Heuvel 1991; Tauris et al. 2017), which includes a common-envelope phase of a giant star with a neutron star companion (Fragos et al. 2019; Law-Smith et al. 2020).

Vigna-Gómez et al. (2020) predicts that only a small fraction ( $\lesssim 1\%$ ) of massive stars ( $\gtrsim 20 M_{\odot}$ ) engaging in a common-envelope phase will become neutron star binaries. However, that study does not incorporate the recently explored stellar evolution models of stripped stars (Appendix A) nor the explosion mechanism explored in this *Letter*. These updates are likely to alter the predicted rates of heavy binary neutron stars and neutron star - light black hole binaries (Section 4.1).

Klencki et al. (2021) used detailed single unperturbed stellar models to explore envelope ejection in massive binaries. They found that heavy ( $\gtrsim 25 M_{\odot}$ ) progenitors with low-mass ( $1 M_{\odot}$ ) companions are not likely to eject the envelope at high ( $\approx$  solar) metallicities. However, it is possible that modeling of progenitors with more massive companions (c.f. their Figure 6), lower metallicities, or different assumptions about energy requirements (Everson et al. 2020), might lead to a successful ejection.

For models considered in this *Letter*, we assumed that the orbit remains effectively unchanged after the envelope ejection. However, the evolution of the post-common-envelope binary can entail energy-momentum losses via stellar winds and tidal dissipation. Assuming that mass is lost via fast isotropic winds, aka the *Jeans* mode, the orbit will widen by a factor of  $\approx 1.7$ . This widening might not result in merging double compact objects for light ( $\approx 1 M_{\odot}$ ) companions, but should not affect the successful merging properties of more massive systems (Figure 4). Moreover, the estimated factor assumes a particular mass loss mode, neglects any the interaction with the companion, and effects such as gravity darkening.

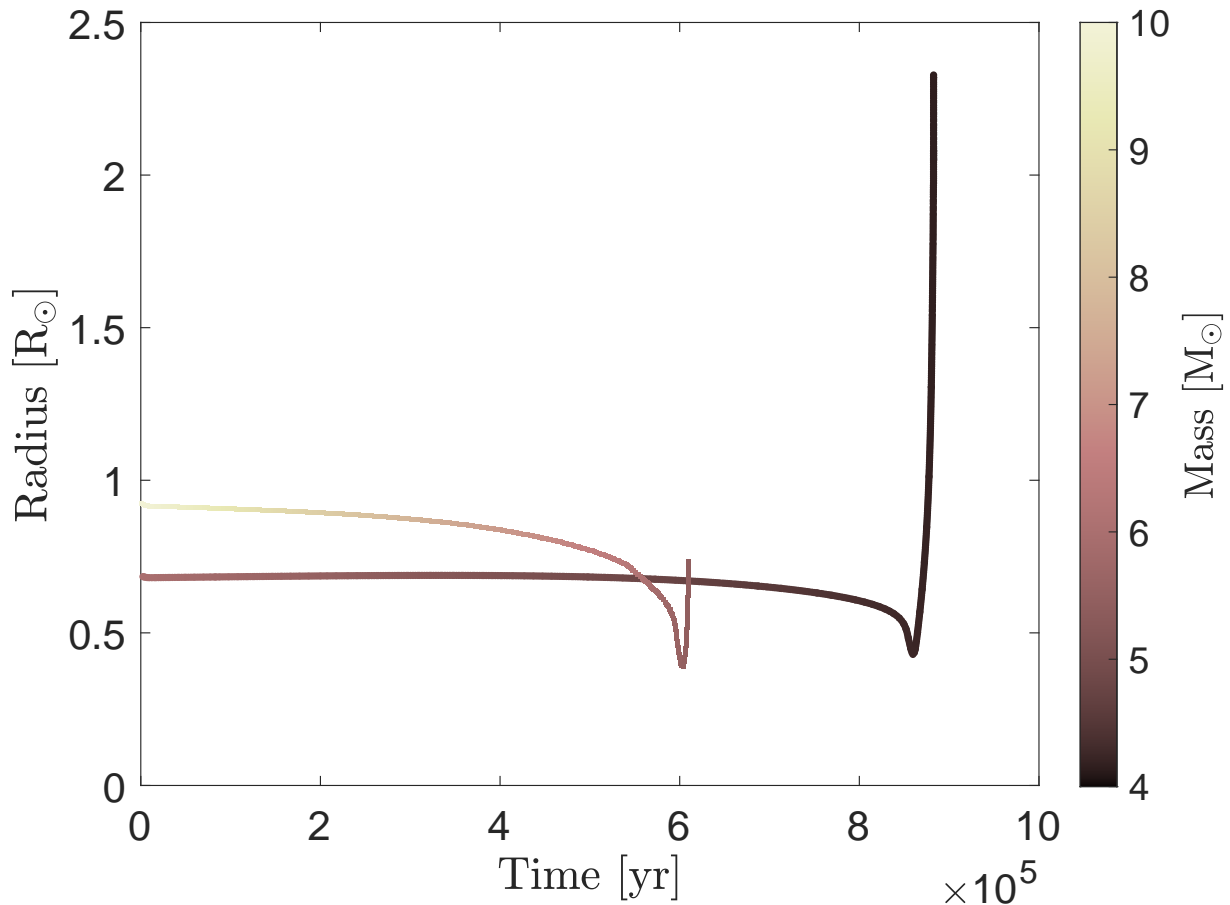


**Figure 6. Time evolution of stripped stars.** Radial (y-axis) and mass (colorbar) time evolution (x-axis) of two helium stars, from helium zero-age main sequence to core collapse, at metallicity  $Z = 0.02$ . The initial helium star masses are 10.0 (initially more expanded) and 6.0 (initially more compact)  $M_{\odot}$ , and reach core collapse with masses of 5.4 and 4.2  $M_{\odot}$ , respectively. The initially more expanded star contracts and the initially more compact star expands.

Additionally, we do not consider tidal dissipation in this study. The dynamical tide is unlikely to play a strong role in the short-lived late stages of binary neutron star assembly, but it might counteract the widening of stellar winds and slightly enhance the merger rate.

### B. 3D HYDRODYNAMICAL SIMULATION OF FALLBACK SUPERNOVAE.

We study the explosion and fallback accretion of a stripped star with a neutron star companion using the 3D Lagrangian hydrodynamic SPH code GADGET-2 (Springel 2005). We use a modified version of GADGET-2 that has been previously used to simulate supernovae in binary black hole forming binaries (Batta et al. 2017; Schröder et al. 2018). Visualization of the hydrodynamical evolution (Figure 2) was made using SPLASH (Price 2007).

#### B.1. Initial conditions and system properties.

Here we describe the initial properties of our fiducial model. The system is initialized as a circular gravitationally bound binary comprised of an exploding star and a neutron star companion at a separation of 1.4  $R_{\odot}$ . The neutron star companion is defined as a sink particle type of mass 1.3  $M_{\odot}$ . In order to build the initial conditions of the exploding star we use a 1D MESA model of a heavy compact progenitor at core collapse (Appendix A). This progenitor, with a helium zero-age main sequence mass of 10.0  $M_{\odot}$  and metallicity of  $Z = 0.02$ , has mass of 5.4  $M_{\odot}$  at core collapse. The star’s final properties at core collapse are then mapped onto a 3D SPH particle distribution that reproduces the density

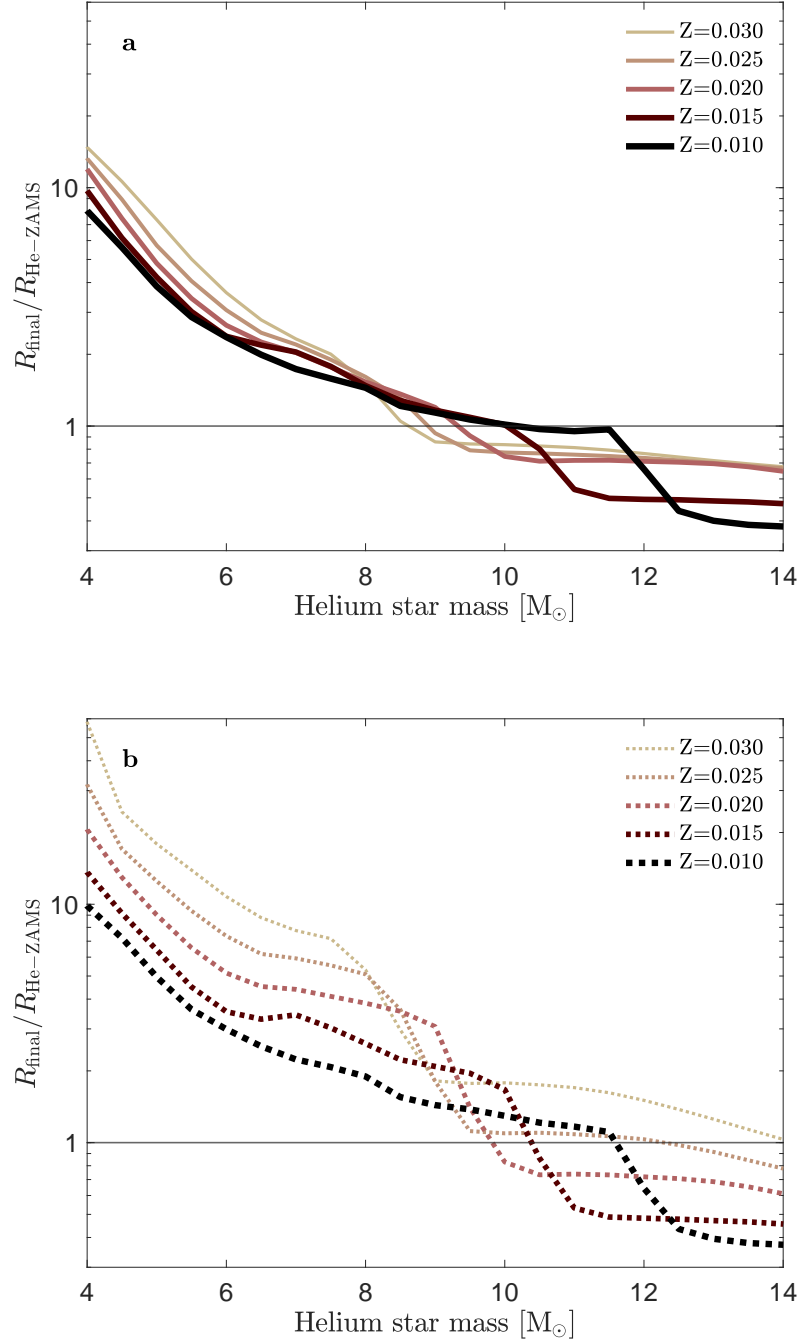


**Figure 7. Summary of radial evolution of stripped helium stars.** The behavior of the radial evolution of stripped stars is shown as a function of helium mass (x-axis) and metallicity (color). We parameterize the radii in terms of  $R_{\text{He-ZAMS}}$  and  $R_{\text{final}}$  (see Methods). Stars remain compact when  $R_{\text{final}}/R_{\text{He-ZAMS}} < 1$ ; alternatively, significant expansion occurs when  $R_{\text{final}}/R_{\text{He-ZAMS}} > 1$ . The results are shown in solid lines (a) for our standard model including `mlt++` and in dashed lines (b) for an alternative numerical treatment of mixing (Appendix A). The former ultimately leads to stars with less extended envelopes at lower masses.

profile. A million SPH particles are uniformly distributed on spherical shells generated with the HEALPix algorithm (Górski et al. 2005). The shells are then spaced according to the local density (Batta et al. 2017). Due to the extremely low densities at the outer layers of the star, mapping with SPH particles became challenging. Therefore, we neglected low density material above  $0.5 R_{\odot}$  resulting in  $\approx 0.1 M_{\odot}$  artificially removed from the system (Figure 5). For the newly born neutron star, the innermost  $1.3 M_{\odot}$  of the 3D stellar structure is removed and replaced by a sink particle with the same mass. For our fiducial model (Figure 2) a kinetic explosion energy of 1.5 bethes is instantaneously deposited in the shell with mass  $dm = 0.7 M_{\odot}$  right above the  $1.3 M_{\odot}$  that comprises the newly born neutron star. We ran a series of models with different explosion energies (Figure 3) spanning from  $0.5 \leq E_{\text{exp}} \leq 4.0$  bethes resulting in different fallback evolution (Figure 8).

### B.2. Resolution study.

We ran simulations for different resolutions to ensure that the remnant mass estimates are accurate for different choices of numerical parameters. For resolutions from  $5 \times 10^5$  to  $5 \times 10^6$  particles we found remnant mass variations smaller than  $0.1 M_{\odot}$  and convergence as the number of particles increases (Figure 9). For our fiducial model we settled for a resolution of  $10^6$  particles resulting in a mass difference of less than  $0.04 M_{\odot}$  compared with the highest resolution. The mass of shell in which the kinetic explosion energy is deposited is the main source of physical and numerical uncertainty. For the  $E_{51} = 1.5$  model, where  $1 E_{51} = 1$  bethe, thin shell masses of  $dm \approx 0.2 M_{\odot}$  lead to remnant masses of  $\approx 3 M_{\odot}$ , more than twice the remnant mass predicted by models which do not incorporate fallback (Müller et al. 2016). Thicker shell masses of  $dm \approx 0.7 M_{\odot}$  converge to more reasonable remnant masses of  $\approx 2.1 M_{\odot}$  (Figure 8). The mapping of 1D stellar models to 3D hydrodynamic ones is known to lead to discretization errors in the hydrostatic equilibrium (Ohlmann et al. 2017). However, the effects of this mapping seem to be negligible in our simulations: while some of the outer layers of the star are artificially ejected because of this, the supernova of a non-exploding model is fully consistent with our lowest explosion energy model, implying complete fallback (see comment about equation of state in Section 4). We lastly checked for any effect that a natal kick could have on the remnant mass. Natal kicks of magnitudes of  $\approx 10$ ,  $\approx 100$ , and,  $\approx 1000 \text{ km s}^{-1}$  at random directions, which affect the orbit in timescales longer than the fallback timescale, made little difference with respect to our fiducial model.

### B.3. Open questions in Supernova Explosion Mechanisms

Supernovae are also very complicated processes to model numerically. We do not present a self-consistent explosion model. Instead, we use a simplified approach to study the long-term evolution of supernova fallback in binaries and explore the sensitivity to the currently unknown supernova energy. This allows us to understand the role of fallback in creating light black holes rather than heavy neutron star pairs. These uncertainties in the explosion energy propagate directly into the rates estimates. Moreover, it is more likely to have a binary remain bound the second explosion lead to a black hole instead of a neutron star (e.g., Figure 4). Future observations will clarify the most likely outcome of stripped supernovae with neutron star companions and will allow us to place strict constraints on the explosion mechanism of massive stars.

Here we follow the model from Batta et al. (2017) in order to quantify the accretion history of the newly born neutron star. We define an accretion radius  $r_{\text{acc}} < 0.01 R_{\odot}$  from the edge of the innermost stable circular orbit (ISCO) of the compact object, in this case the  $1.3 M_{\odot}$  proto-neutron-star. Particles within the accretion radius and with less specific angular momentum ( $j$ ) than the one needed to orbit ISCO are considered to be accreted, transferring their entire mass and angular momentum onto the compact object. Particles within the accretion radius and with  $j_{\text{ISCO}} \leq j < 10 \times j_{\text{ISCO}}$  are assumed to be accreted via an accretion disk on a viscous timescale. To this end we neglect any additional feedback from this accretion.

## C. POPULATION SYNTHESIS OF STRIPPED STARS.

We perform a population study of massive binary stars using the rapid population synthesis element of the COMPAS (Stevenson et al. 2017; Vigna-Gómez et al. 2018) suite v02.19.01. We do this to estimate order-of-magnitude formation rates for these systems. We simulate  $10^7$  massive binaries ( $M > 5 M_{\odot}$ ) at representative metallicities  $Z = \{0.02, 0.0142, 0.01, 0.001, 0.0001\}$  following the setup from Vigna-Gómez et al. (2020). The data is publicly available and can be found in [zenodo.org/record/4682798](https://zenodo.org/record/4682798) (Vigna-Gómez et al. 2021). We focus on the onset of Roche lobe overflow leading to a common-envelope phase for systems with a neutron star companion. This configuration is the immediate progenitor of the stripped star we model in MESA; i.e., we expect that the post-common-envelope star will

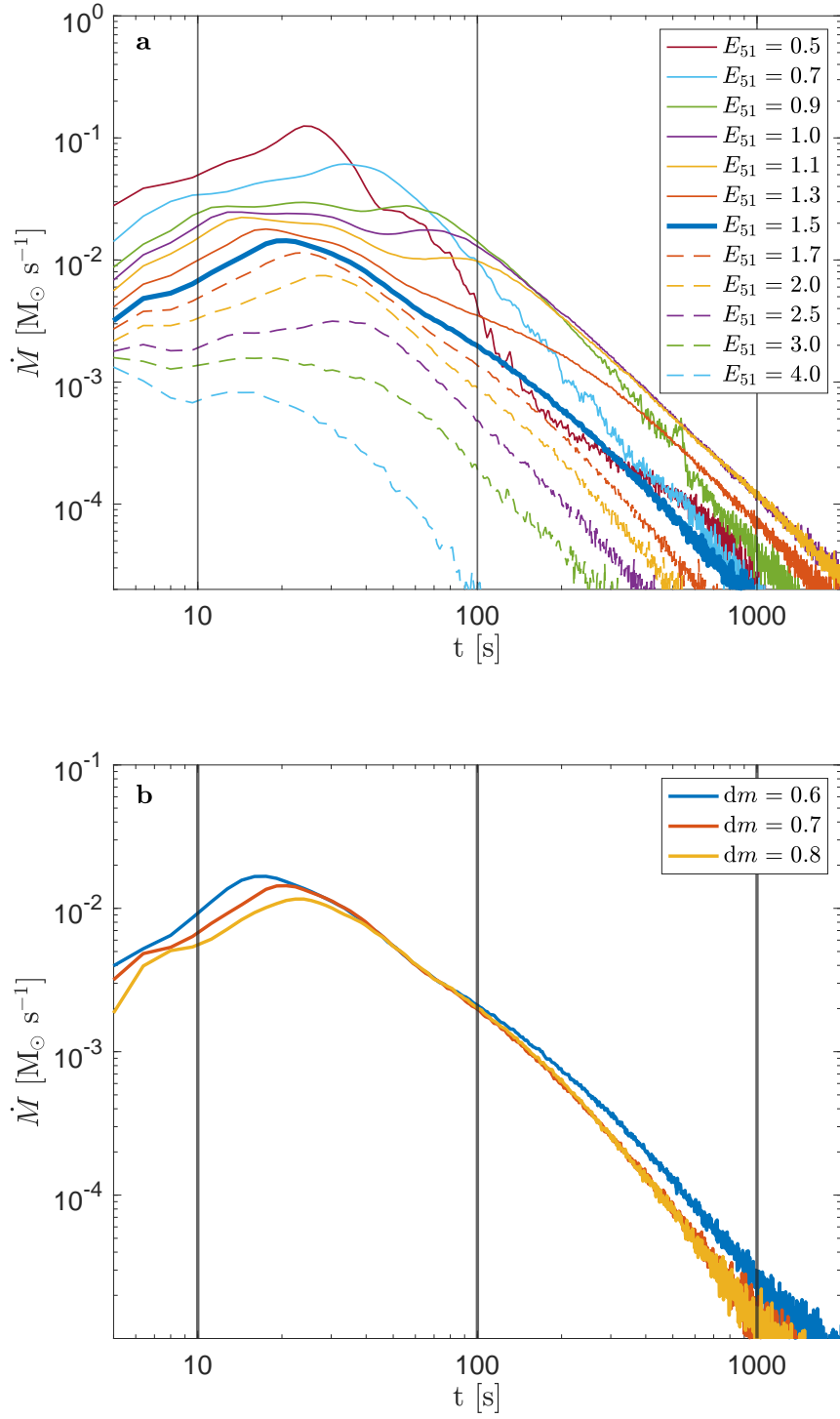


**Figure 8. Fallback mass accretion rate of the exploding star.** All models (a) and resolution study (b) exploring the evolution depending on the size of the mass shell where the kinetic explosion energy is deposited (Appendix B).



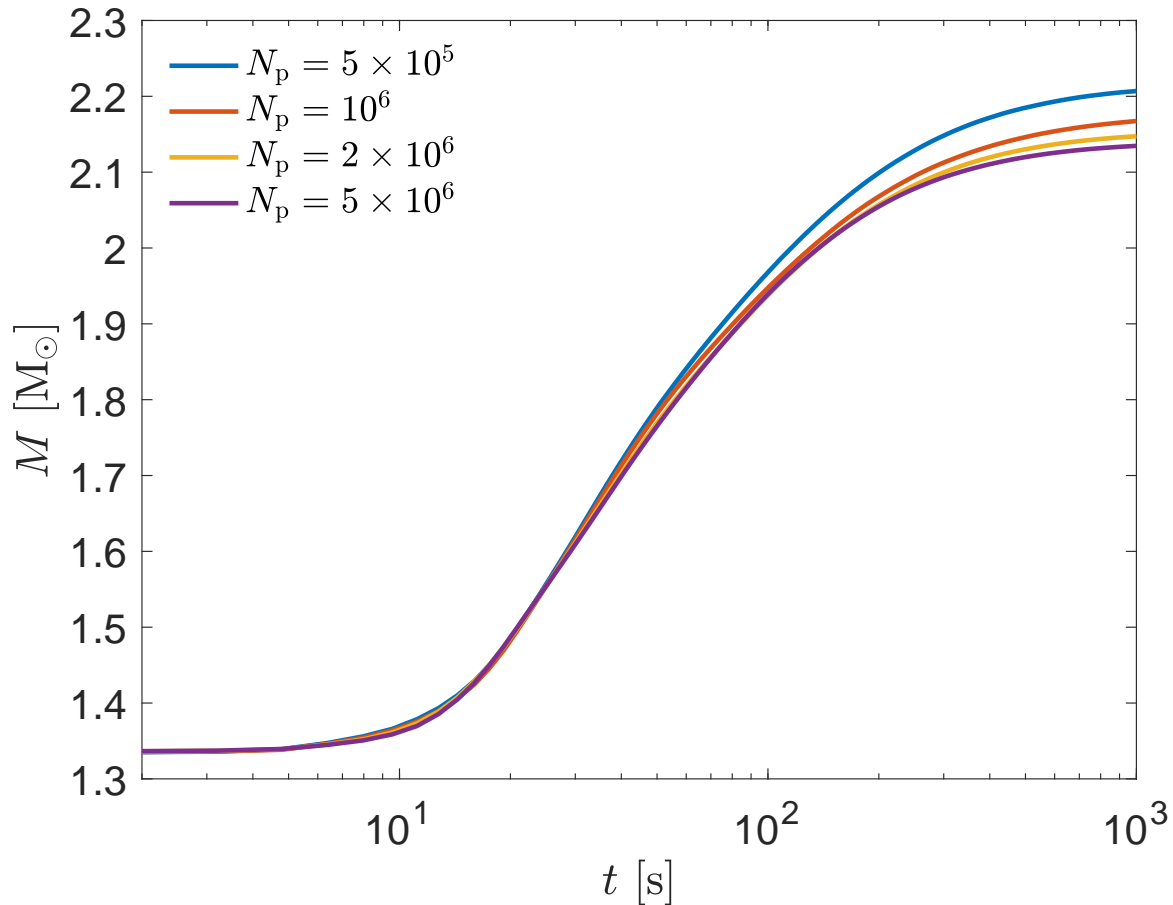


**Figure 9. Post-supernova time evolution, including mass accretion, of the newly born neutron star.** Number of particle ( $N_p$ ) resolution study to determine convergence in our simulations (Appendix B).

evolve as a stripped star. We remain agnostic about the evolution and outcome of the common envelope phase and present all systems that arrive to this phase, regardless of the post-common-envelope evolution in COMPAS. Therefore, our rate estimates include Thorne–Zytkow objects (Thorne & Zytkow 1975, 1977), merging and non-merging heavy binary neutron stars, and merging and non-merging neutron star - light black hole binaries. We use the core mass at the onset of the common-envelope phase as a proxy for the stripped helium star mass and show both the cumulative distribution function and yield, that is the number of systems of interest per unit star forming mass, at each metallicity (Figure 10). The yields of these events, which could be observable as bright luminous red novae (Howitt et al. 2020; Vigna-Gómez et al. 2020), is several times  $10^{-5} M_{\odot}^{-1}$  at any given metallicity. Depending on the lower mass threshold that leads to the bifurcation between expanding and contracting envelopes, the formation rate can increase by a factor of  $\approx 2$ . This estimate serves as an upper limit on the birth rates of heavy binary neutron stars. For a Milky Way galaxy with a continuous star formation rate of  $2 M_{\odot} \text{ yr}^{-1}$  (Chomiuk & Povich 2011), the assembly rate of potential heavy stripped stars with a neutron star companion is  $\approx 100 \text{ Myr}^{-1}$  or 0.01 per local core-collapse supernova.

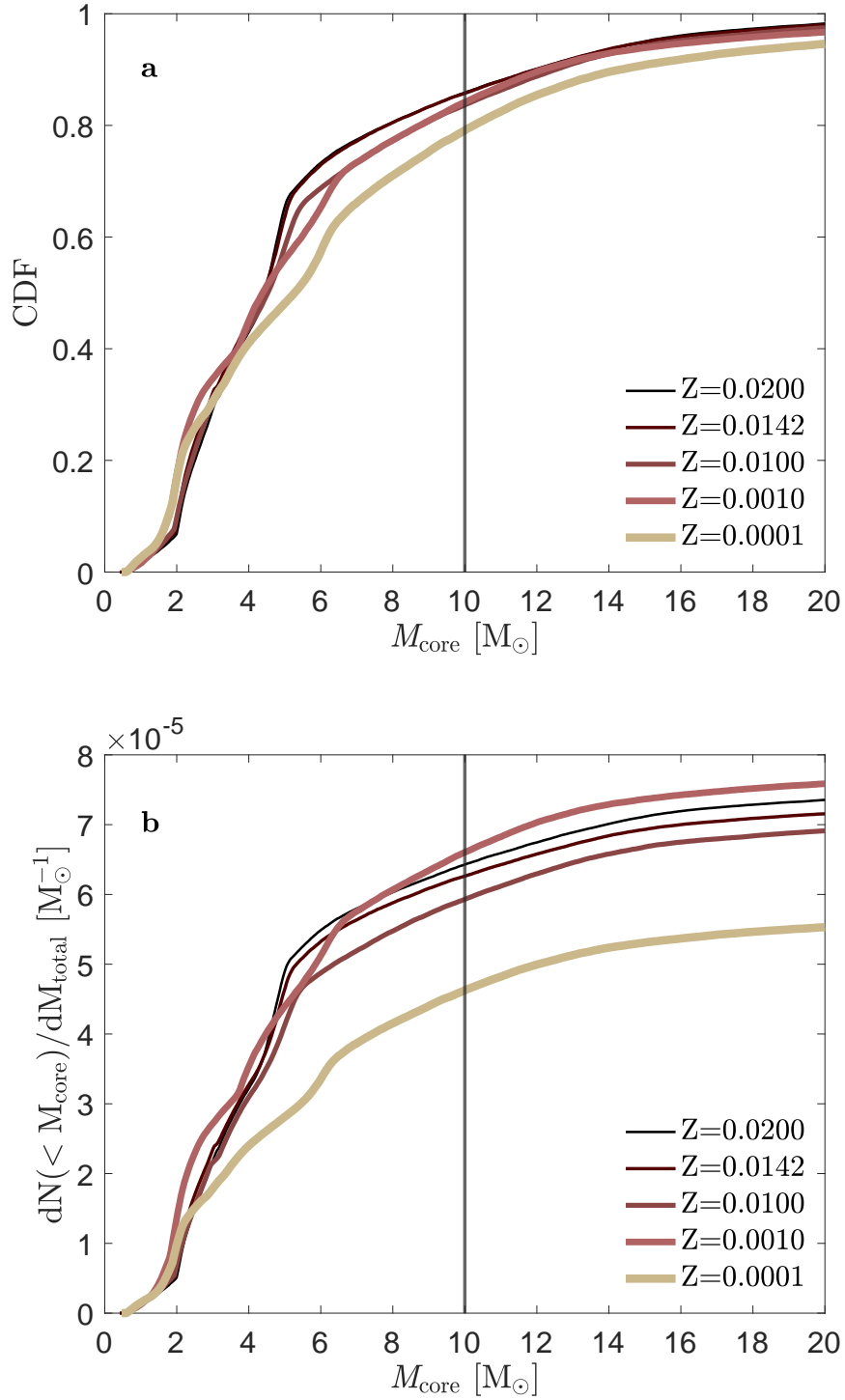


**Figure 10. Population synthesis of stripped stars with a neutron star companion.** Cumulative distribution function (a) and yields (b) of the core mass of stars with a neutron star companion at the onset of Roche-lobe overflow leading to a common-envelope event. After stripping, the mass of the helium star will be similar to this core mass. Stripped stars with mass  $\approx 10 M_{\odot}$  will remain compact throughout their evolution and lead to heavy binary neutron stars. More massive stripped stars are predicted progenitors of neutron star - light black hole binaries.